Available online at www.sciencedirect.com
ScienceDirect
Tetrahedron 63 (2007) 7366–7374
Tetrahedron

Rheometry of an androstanol steroid derivative paramagnetic organogel. Methodology for a comparison with a fatty acid organogel

Pierre Terech* and Séverine Friol

UMR5819 CEA-CNRS-Univ. J. Fourier, DRFMC-SI3M-PCM, CEA-Grenoble 17, rue des Martyrs, 38054 Grenoble Cedex 9, France

Received 30 October 2006; revised 5 February 2007; accepted 9 February 2007
Available online 20 February 2007

Abstract—This paper compares and contrasts the behavior of two different gelators using rheological and neutron scattering methods. The flow properties of a steroid-made paramagnetic organogel in cyclohexane are presented. The original gelator **STNO** is important in the class of organogels as being one of the most documented and as such is a good candidate for comparisons with another reference system, the 12-hydroxy stearic acid (**HSA**) gel. The linear viscoelastic regime of deformations of **STNO** gels is identified and analyzed in the context of self-assembled fibrillar networks. The linear elasticity scales with the concentration as $G' \alpha C^2$ similarly with **HSA** organogels, and both systems can be considered as cellular materials. Rheological and neutron scattering experiments show that the kinetics of gel formation exhibits long equilibration times corresponding to the elaboration of entangled fibrillar aggregates. Comparison of the linear elasticities between **STNO** and **HSA** gels demonstrates that **HSA** gels are much more stiffer ($G'_{HSA}/G'_{STNO} \sim 2700$). Contributions from the cross-sectional sizes, the mesh size of the networks, the solubility concentrations, and the Young's modulus of the materials are discussed. Non-linear flow properties are also compared using thixotropic loops. They indicate that the transduction of the chirality from the molecular to the supramolecular stages is more efficient with **STNO** gels having strong chiral junction zones. Simplified scattering and optical protocols are proposed to facilitate comparisons between different organogels.

1. Introduction

Molecular gels[1–3] form a special class of gels beside polymer gels and mineral systems.[4] Their basic characteristic features are: (1) formation from low-mass molecules, (2) thermoreversible sol to gel phase transition, (3) low concentration of active gelator molecules (in the range 0.1–1%). The rational investigation of these materials started in the 1970s mainly with the contribution of Tachibana et al. exploring the 12-hydroxy stearic acid (**HSA**) organogels (Scheme 1).[5–7] In the following decade, Terech et al. initiated a period characterized by the introduction of new techniques such as small-angle neutron scattering (SANS),[8] cryo transmission electron microscopy (TEM),[9] and electron paramagnetic resonance (EPR)[10] as applied to a steroid-made molecular organogel. The development of fundamental research on molecular gels was then supported by a great input from chemists of different groups.[11–15] The quest for chemical design rules controlling the gelating ability motivated these efforts: this difficult molecular engineering challenge remains out of reach in most cases. On the other hand, the explored distances using physical techniques now range from the atomic level with crystallographic studies of the molecular arrangement in the fibers[3,16,17] to the nanoscopic scale with the determination of the global morphology of the fibers and associated networks (scattering and electron microscopy methods). Molecular aggregation mechanisms can hence be proposed for an increasing number of systems.[3] On the macroscopic scale, investigations usually focus on the remarkable viscoelasticity of the supramolecular systems. Nevertheless, rheometry applied to molecular gels has to take into account of the particular fragility of the systems, arising from the self-assembled nature of the self-assembled fibrillar networks (SAFINs) made up of low-mass molecules, and their sensitivity to statistical parameters governing the one-dimensional (1D) crystalline growth through nucleation mechanisms. An important step for the elaboration of the physical and chemical concepts appropriate to describe SAFINs in molecular gels now becomes the comparison of the properties between different systems. In particular, multiple correlations might be expected between the molecular aggregation mechanisms involved in the fibrillar growth, the specific Young's modulus of the resulting fibers, their cross-sectional shapes and sizes, their bending rigidity, the mesh size of the networks, and the macroscopic elasticity of the gels.

Keywords: Organogels; Rheology; Steroid; Neutron scattering.
* Corresponding author. Tel.: +33 4 38 78 59 98; fax: +33 4 38 78 56 91; e-mail: pierre.terech@cea.fr

0040–4020/$ - see front matter © 2007 Elsevier Ltd. All rights reserved.
doi:10.1016/j.tet.2007.02.067

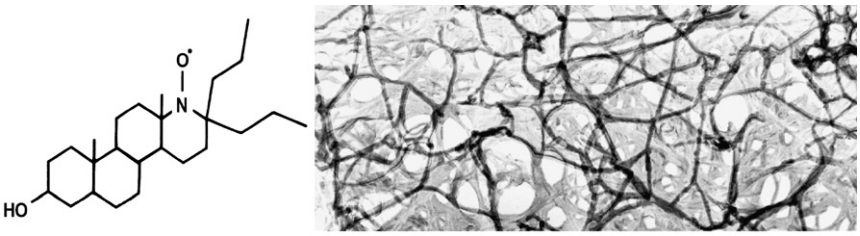

STNO

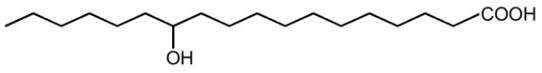

HSA

Scheme 1. Chemical structure of **STNO**, a paramagnetic D-homosteroidal nitroxide free radical (D-3β-hydroxy-17,17-dipropyl-17a-azahomoandrostanyl-17a-oxy). Corresponding transmission electron micrograph view of the **STNO** SAFIN (C∼2 wt %). The finest fibers have ca. 120 Å diameter. Chemical structure of the 12-hydroxy stearic acid **HSA** organogelator.

We report on a selection of rheological properties of a steroid-made paramagnetic organogel (**STNO**) in cyclohexane. The system is well documented as being the first molecular gel for which systematic physical studies have been undertaken and is a model system considering the time stability of the gels (at least several years), their optical transparency, the capacity of growing crystalline single crystals in non-gelling solvents, the helical features at the nanoscale, etc. The situation is thus ideal to attempt a rheological comparison with the reference system **HSA**. The requirements and limitations of the development of such an approach are also analyzed in this paper.

2. Results and discussion

2.1. The complex nature of SAFINs

SAFINs form the solid-like component of molecular gels, which can be considered as biphasic systems. The dispersion degree of the SAFIN (C<1 wt %) is such that the gels can appear as transparent and stable systems. The three-dimensional (3D) infinite network spans the entire macroscopic volume involving a variable degree of entanglement of 1D species. The actual composition of SAFINs can be complex and mix variable volume fractions of fibers, of zones where they join, but also of nanocrystallites that can develop within the confinement provided by the opened cells of overlapped fibers. Moreover, different morphs can coexist both in the fibers and the heterogeneities forming the solid part of the gel network. At the end, the specificity of molecular gels is such that some of the parameters representative of SAFINs can be *strictly determined* (i.e., cross-sectional sizes of the fibers, molecular aggregation mechanism) while others can be *statistically averaged* (i.e., volume fraction of gelator in the SAFIN) and others remain *undetermined* (i.e., fiber trajectory, large-scale distribution of the heterogeneities). The statistical nature of the 1D growth of low-mass molecules intrinsically accounts for the usual delicate reproducibility of absolute rheological measurements. Scheme 1 shows a transmission electron micrograph of a **STNO** SAFIN. The topography is strongly dependent on the preparation protocol and some aspects (i.e., number densities of fibers and junction zones) can directly affect the viscoelastic properties and time stability of the gels. Although the equilibrium state of molecular gels remains the phase-separated solid–liquid state, the time stability (which is very system-dependent) can be quite favorable (>years). The particular pattern proposed by molecular gels emphasizes the need for a suitable theoretical framework balancing solubilization (or micellization) and crystallization processes, by 'adjusting' physical concepts used for polymeric systems in solution with those used for surfactants in solution.

With rheometry, any experimental protocol should take into account of the sensitivity of the SAFINs to their rheological history, of the protocol used for the gel deposition/formation into the gap of the rheometer and of the long relaxation times associated with the hampered translational diffusion of 1D species in networks. As a result, a refined protocol combining a series of experiments must provide a statistical error on the elastic shear modulus G'<20%. In such a context, the objective(s) of the rheometry applied to molecular gels need(s) to be clarified. First, rheometry can be used 'primarily' to qualify the system as a gel through its viscoelastic response, which should be typical of a soft solid (G'/G''∼5–10 over 10^{-4}–100 Hz frequency range of the oscillatory applied stress). In the course of such studies, the identification of more sophisticated behaviors using G', G'' versus frequency experiments may occur, and the discovery of breakable supramolecular polymers,[18] suspensions of finite aggregates,[19] or other systems such as mesogels,[20] rod gels,[21] ringing gels,[22] and other soft glassy materials[23] cannot be excluded. Second, the determination of the scaling laws of G', G'', and yield stress σ^* with concentration and the theoretical analysis of the exponents are major steps in the understanding of the deformation of the SAFINs.[24] Third, comparing the absolute values of the elasticities, viscosities, and scaling exponents of various systems is now a pre-requisite to derive general rules and concepts for this class of gels.

2.2. Rheology of STNO–cyclohexane organogels

The steroid-made organogels were historically among the very first[25,26] for which a collection of structural data was

extracted from TEM, SANS, optical microscopy, DSC, IR, and WAXS (wide-angle X-ray scattering for crystallographic analyses). To summarize, the **STNO/STNH** network is made up of rigid helical fibers with diameters ranging from 100 to 175 Å depending on the type of apolar organic liquid in which they are generated. The cohesiveness of the fibers is due to the growth of infinite sequences of H-bonds parallel to the fiber axis. The paramagnetic character of the **STNO** gelator has allowed the accurate extraction of the phase diagram[10] as well as a first analysis of its kinetics of growth.[27] X-ray crystallography using a high resolution powder diffractometer operating with a brilliant synchrotron source and 'direct-spaces' approaches are in progress to resolve the molecular structure in xerogels and gels.[28] At the other end of the length scale, the standard rheometry technique is probing over millimeter distances how the mechanical parameters of the individual fibers such as the bending and stretching elastic moduli (and potentially other components i.e., twist and splay moduli in chiral systems) are transduced to the macroscopic elasticity. We present selected rheological data concerning **STNO**–cyclohexane organogels that were missing in the description of the model system. The investigation is conducted to ultimately compare directly with the flow characteristics of the **HSA**–cyclohexane system.

First, the linear viscoelastic regime (LVE) of deformations in an oscillatory shearing mode is a regime of small amplitude straining that can be expressed as in Eq. 1[29] and constitutes the pre-requisite for a quantitative study.

$$\sigma(t) = \gamma_0[G'(\omega t)\sin(\omega t) + G''(\omega t)\cos(\omega t)] \quad (1)$$

It is important to realize that the complex nature of the SAFINs (vide supra) may hamper the existence of the LVE regime. The quality of the LVE domain determines the reproducibility of the measurements. Special attention is thus paid to its determination. Figure 1A shows that linear parts in the logarithmic representations of G' versus stress curves can be identified (see for instance, at C=0.5 wt %, stress σ<688 Pa while at C=6 wt %, σ<38511 Pa). The logarithmic representation G' versus strain γ (Fig. 1B) indicates an apparent LVE domain for **STNO** SAFINs defined as a deformation range 0.006<LVE<0.0035 in the concentration domain 0.5 wt %<C<6 wt %. Nevertheless, the examination of the semi-log representation of G' versus γ (Fig. 1C) already shows some alterations of the apparent LVE domain. The LVE extension is limited to very weak deformations and characterizes a rigidly connected network. Figure 1C shows the occurrence of limited and partial strain hardening. The increase of the LVE domain with concentration is a feature that might be, as a first step, accounted for by the theoretical context of colloidal gels formed of interacting flocs.[30] In such a model, depending on the relative strength of the inter- and intra-floc links, several regimes can be defined. Theoretically, an increase of the domain of linearity with concentration should reveal a weak-link regime. On the contrary, in a strong-link regime the elasticity of the gel results from the elasticity of the flocs. It will be shown that the description of the **STNO** gel architecture does not require the packing of fractal-like flocs. More consistently, the deformation of the **STNO**–cyclohexane energetic network of fibers results from the strain of a homogeneous and continuous

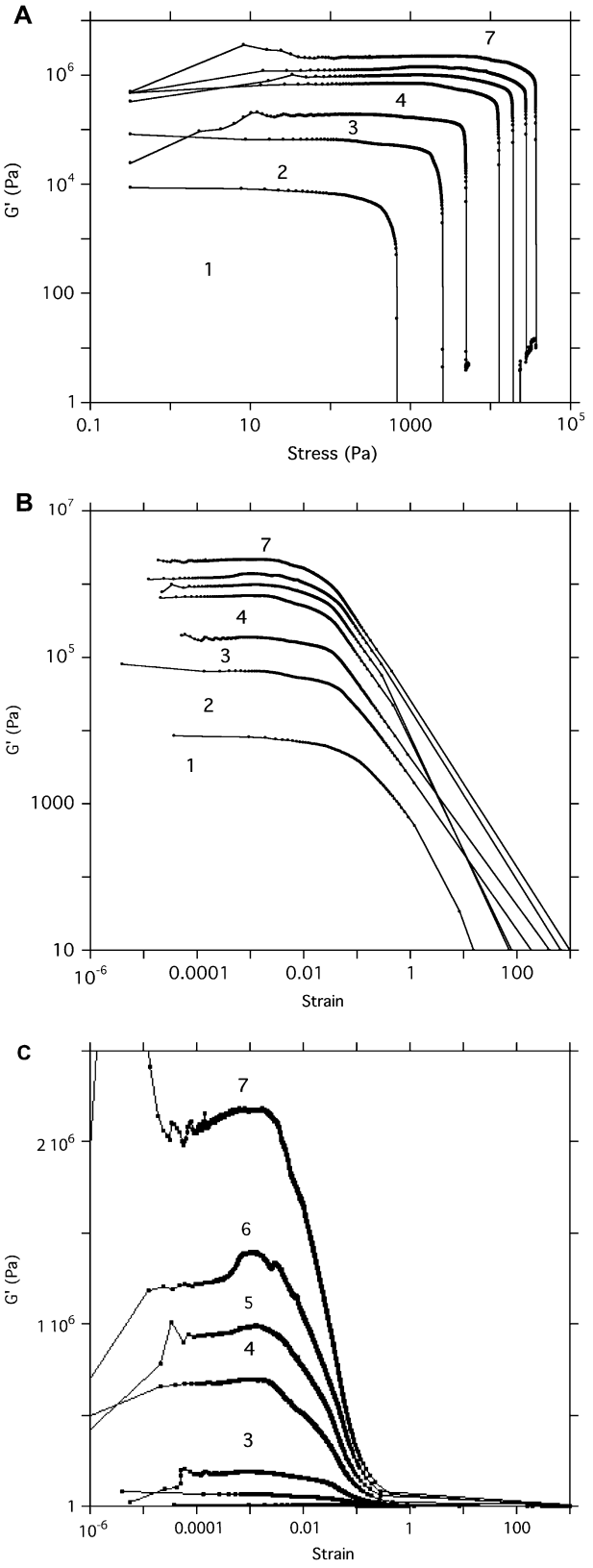

Figure 1. Graphic representations for the search of the linear viscoelastic regime of deformations in the **STNO**–cyclohexane molecular organogel. An oscillatory (1 Hz) stress ramp is applied for samples of concentrations **1**: C=0.5 wt %, **2**: C=1.0 wt %, **3**: C=2.0 wt %, **4**: C=3.0 wt %, **5**: C=4.0 wt %, **6**: C=5.0 wt %, **7**: C=6.0 wt %. (A) G' versus stress curve, log–log scale. (B) G' versus strain curve, log–log scale. (C) G' versus strain curve, semi-log scale.

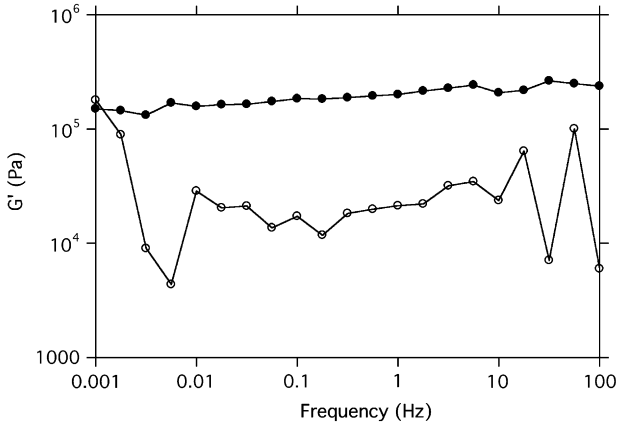

Figure 2. Example of a frequency sweep curve (G', G'' versus frequency) for a **STNO**–cyclohexane gel at C=2 wt % at σ=5 Pa.

distribution of cells. The amplitude of the G' variations in the apparent LVE is <20% and is assumed acceptable for further rheological investigations.

Figure 2 shows the frequency (ν) profile of G' in the LVE regime. At ν=1 Hz, $|G'/G''|\sim 9$ as expected for a soft viscoelastic solid like a gel. The G'' profile is more erratic, as frequently observed with SAFINs, but does not show any feature that would characterize a slow and specific viscoelastic relaxation mode. Actually, the departure of G' versus ν from a strict plateau suggests that other relaxation modes are nevertheless operative in the SAFINs (in particular at much longer times). The weak frequency dependency of G' and G'' has no influence on the scaling laws extracted at ν=1 Hz. Because the quality of the LVE regime is acceptable, the reproducibility of the measurements is then tractable using stress sweep experiments undertaken for a series of seven concentrations with a minimum of five different trials for each of them (corresponding to fresh sample loads in the gap of the rheometer). Figure 3 shows the scaling laws for the elastic shear modulus G' and the yield stress σ^* values:

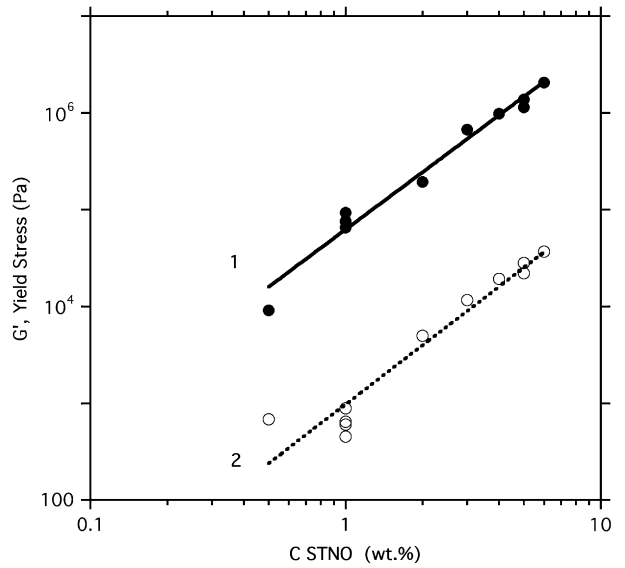

Figure 3. Scaling laws of G' and σ^* versus concentration for **STNO**–cyclohexane organogels: $G'\sim 62051C^{1.96}$ Pa and $\sigma^*\sim 969^{2.02}$ Pa.

the exponents are 1.96 and 2.02, respectively. The similarity of the exponents on both G' and σ^* suggests the similarity of the mechanism of rupture in the networks for which the relationship $\sigma^*=\gamma_c G'$ can apply. Nevertheless, this remark does not prejudge the way that, under a given deformation, the energy is stored in bending and stretching modes of the fibers. The refined examination of how much affine is the deformation field in such networks[31] remains to be undertaken but is beyond the scope of the present global analysis.

The value of the exponent (ca. 2.0) can be classically interpreted in the theoretical context of cellular solids.[32,33] The network is modeled as unit cells staggered with fibers at their midpoints. The network is considered to be an energetic network that can be deformed only by bending its fibers. Some entropy can still be introduced by allowing rotation of the fibers in the 'crosslink zones'.[34] These zones are microcrystalline domains characterized by Bragg peaks at large Q values (not shown). The scaling exponent of 2.0 suggests that the fibers are rigidly connected to each other. It is known that self-assembled 1D species are actually semi-rigid or rigid structures and persistence lengths of the order of microns are frequently observed in these gels.[3] As mentioned above, the deformation in SAFINs is a complex matter that will certainly take advantage of theoretical models developed for rigid biological systems where correlations at distances larger than the mesh size are considered.[35]

Values of the macroscopic elasticities stringently determined as described above can now be compared to those of other molecular organogels. Figure 4 illustrates such a comparison with the **HSA** system.[36] The difference in the scaling exponents (2.22 and 1.96 for **HSA** and **STNO**, respectively) is not significant enough to consider a different theoretical framework[35] (a $G'=C^{-1.96}$ variation is shown in Figure 4 to evaluate the difference). The intersects of the power law

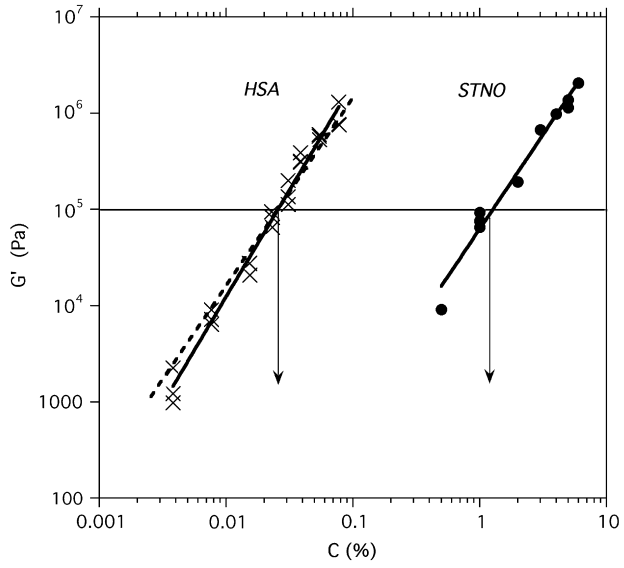

Figure 4. Methodology for a comparison of the flow properties between two different organogels: G' versus C scaling laws (bold straight lines) of **STNO**–cyclohexane and **HSA**–dodecane organogels (see paragraph discussion) are shown. The dotted straight line has a slope equal to 1.96. The intersections with the horizontal straight line at $G'=10^5$ Pa relate to the corresponding concentrations of the two gelators (see arrows).

variations with an horizontal line at G'=100,000 Pa provide concentration correspondences at C=0.026% for a **HSA**–dodecane gel and C=1.196% for a **STNO**–cyclohexane gel. Strictly, only the effective gelator concentration $C=C_0-C_g$ should be considered (with C_0 being the initial concentration and C_g the critical gelation concentration at which the SAFIN and gel are formed). The choice of the most appropriate concentration to take into account is not trivial between the *cmc* (critical micellar concentration), the C_{ag} (critical aggregation concentration) at which finite 1D aggregates of the sol phase are formed, and the C_g (gelation concentration). Beyond C_{ag}, elastic aggregates are present that may contribute to the macroscopic elasticity. By contrast, C_g is certainly an overestimated value. Half the C_g values (0.005 wt % for **HSA** and ca. 0.35 wt % for **STNO**) can be reasonable choices. The ratio of corrected concentrations ($C_0-C_g/2$) for the two systems (at ν=1 Hz and T=20 °C) is **STNO/HSA**~40. It indicates that a much higher concentration of **STNO** is required to produce elasticities of the level of those for **HSA** gels. A different way of comparing the systems is to consider the elasticities at a fixed concentration (i.e., 1 wt %). This gives $G'_{STNO}\sim 6\times10^4$ Pa, while $G'_{HSA}\sim 1.6\times10^8$ Pa. A first conclusion is that **HSA** organogels in cyclohexane are very much stiffer than those constructed from the steroid! The origin of the difference ($G'_{HSA}/G'_{STNO}\sim 2.7\times10^3$) can be considered on the basis of the Young's or elastic modulus of a network (expression 2).

$$E=\sigma/\varepsilon=kE_s(D/L)^4 \tag{2}$$

D is the diameter of the fibers, L is their length (which can also define the mesh size ξ of a regular and ideally homogeneous network), and E_s is the stiffness of the constitutive material.

Thus, three potential sources for the differences in the measured elasticities can be identified. First, the intrinsic stiffness of the aggregated gelators can be related to the energy of scission of the fibers. The cohesiveness of a fiber is related to the number of connections per gelator molecule and the number of molecules associated per unit length of fiber. Crystallographic analyses of the molecular structures in the gel fibers can provide clues for this contribution. Second, differences in the sizes of the cross-sections of the fibers (expression 2) contribute significantly to the differences in the gel elasticities. The small-angle scattering technique is a non-invasive technique that has proved to be suitable to extract such structural features on the nanoscale. The contribution of the cross-sectional sizes to the resultant elasticity can be evaluated by SANS experiments. Figure 5 compares the scattering curves of **HSA** and **STNO** organogels in deuterated cyclohexane at comparable concentrations. Expression 3a describes the form-factor intensity decay at low Q values for fibers with elliptical cross-sections ($e=b/a$, with b being half the small side and a half the large axis). For e=1, the expression reduces to that for circular cross-sections.

$$I(Q\to0)\to\frac{\pi}{Q}\left[1-\frac{Q^2a^2}{8}\left(1+e^2\right)\right] \tag{3a}$$

$$I(Q\to\infty)\to(\Delta\rho)\frac{2\pi}{Q^4}S \tag{3b}$$

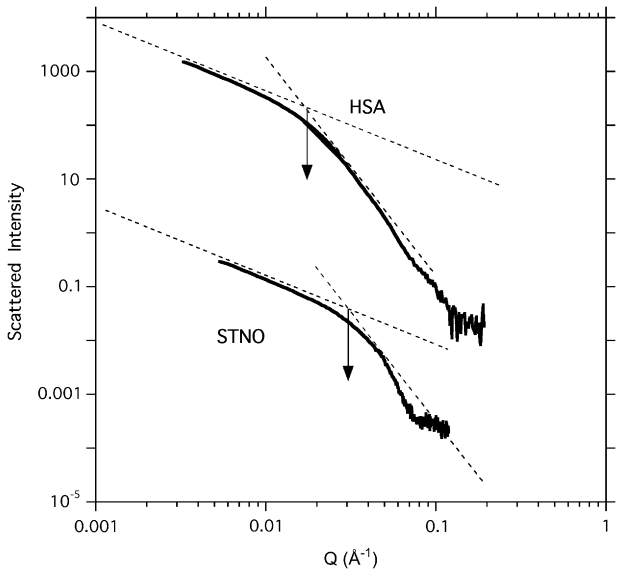

Figure 5. SANS curves for **STNO** (C=2.55 wt %) and **HSA** (C=1.4 wt %) in deuterated cyclohexane in the Q range appropriate for a rapid estimation of the cross-sectional areas of the fibers forming the SAFINs. Arrows point at the intercepts Q^* between the large ($dI/dQ=-4$) and low Q asymptotic ($dI/dQ=-1$) behaviors (dotted lines).

To compare efficiently and conveniently the different systems, a fast method is required. For this reason, the refined analytical method[37] detailing the scattering data is not considered here and a simplified approach is preferred. Figure 5 proposes to extract a Q value (Q^*) characteristic of the cross-sectional area of the 1D scatterers. Q^* is defined by the intersection between the low Q asymptotic intensity decay typical of 1D aggregates (theoretically Q^{-1}) and the Q^{-4} decay typical of the scattering by their interface at large Q values (expression 3b). It is found that for **HSA**, $Q^*\sim$ 0.01744 Å^{-1} while for **STNO**, $Q^*\sim$0.0304 Å^{-1}. The corresponding cross-sectional areas are roughly in the ratio $A_{HSA}/A_{STNO}\sim(0.0304/0.01744)^2\sim3.0$ assuming circular cross-sections. The method is only indicative and cannot replace the refined analysis in particular if non-identical and anisotropic cross-sectional shapes are involved. It has been shown[38] that slightly anisotropic ribbons ($A_{HSA}\sim150\times300$=45,000 Å^2) are formed for **HSA** in cyclohexane[36] while with **STNO**, the average area[8] was $A_{STNO}=130\times130$=17,000 Å^2 giving a ratio $A_{HSA}/A_{STNO}\sim2.7$ close to the estimated value of 3.0. Following expression 2, the differences in the cross-section sizes account for a variation in the elasticities such as $E_{HSA}\sim10\,E_{STNO}$.

Finally (and third), the average mesh size ξ of the distribution of fibers in the networks is also a determining parameter (see expression 2) and questions the exact composition of the SAFINs. The larger the proportion of junction zones and heterogeneities, the larger will be the average mesh size of the heterogeneous network. The volume fraction and homogeneity of the networks are parameters difficult to extract. A single example, using scattering techniques in favorable scattering conditions (decoupling between the form and structure factors), has estimated the fraction of nodes in bile-acid derivative hydrogels.[24] Here, the data suggest that at a similar active concentration, the **HSA** network has a smaller mesh size than **STNO** and in the proportion

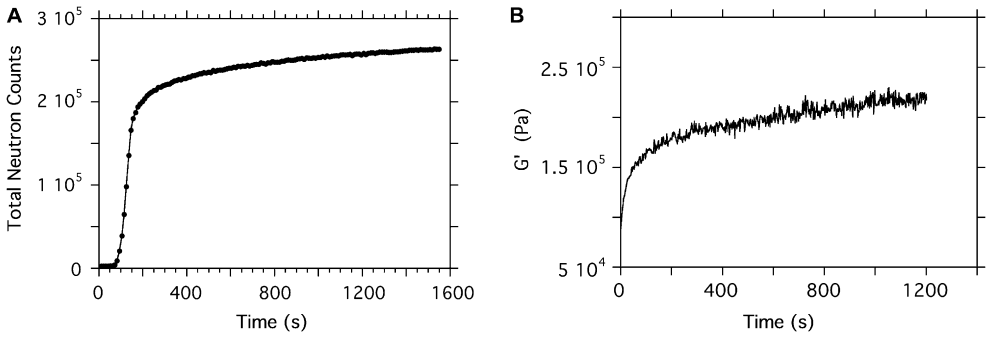

Figure 6. Kinetics of SAFIN's growth in a **STNO**–cyclohexane gel. (A) SANS experiment at C=2.55 wt %. (B) Rheometry at C=2.0 wt %, ν=1 Hz, σ=5 Pa). The inset is a semi-log plot that illustrates the caution required for the identification of a true stabilized state.

$\xi_{STNO}/\xi_{HSA} \sim \sqrt[4]{270} \sim 4$. Assuming a similar persistence length and stiffness for **HSA** and **STNO** fibers, this would indicate that most of the **HSA** gelator in cyclohexane gels is involved in the growth of fibers rather than in a micellization process or in the formation of bundles or other heterogeneities.

The analysis of the kinetics of formation can also provide a valuable piece of information for the comparison of gels. The kinetic process is known to result from an apparent two-step sequence.[27] The first step is very fast with a kinetic order $n \geq 2$ while the final step exhibits a kinetic order ≤ 1. Therefore, the equilibrium state can only be reached after a long period of time. This specificity can also be a determinant for the experimental reproducibility of the rheological and structural measurements. Figure 6 shows that SANS and rheometry are convergent techniques to characterize such long equilibrium times. The corresponding data confirm that the rheological signature is directly related to the increase of the number density of growing **STNO** fibers and not to re-ordering processes of the networks. A typical kinetic time $\tau_{1/2}$ of the sharp rheological or scattering sigmoid variation is ca. 70 s (C=2.5 wt %) while the terminal plateau is reached after $\Delta t > 3600$ s. A comparison with **HSA** indicates that the initial step is similarly fast but the equilibration is more quickly reached ($\Delta t < 2000$ s, not shown). The relation between the complexity of the molecular aggregation mechanism and the kinetics is not straightforward. At this stage, it can be noted that chirality is a driving force for the **STNO** aggregation for which helical fibrils involved in double helixes have been identified by TEM measurements.[9] With **HSA**, although the molecule is chiral, the importance of chirality at a supramolecular level is attenuated since the gel can be formed in both chiral and racemic situations.[38] The time required for reaching the equilibrium is related to the depth of the well of potential energy corresponding to the aggregated state. This also indicates the high level of thermodynamic instability of the isolated **HSA** molecules compared to that for **STNO** when put in supersaturated conditions.

A last step in the comparison of the mechanical properties of SAFINs can be the monitoring of their thixotropic properties. For stress values larger than those corresponding to the end of the LVE regime and lower than the yield stress σ^* (at which the network is ruptured), a creeping process develops that can be used for direct comparisons of gels. Figure 7 shows thixotropic loops observed for ascending stress ramps followed immediately by descending stress ramps. The method is

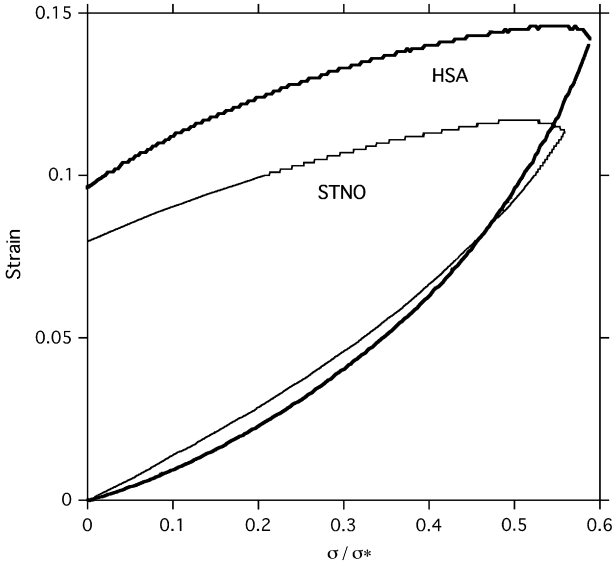

Figure 7. Comparison of the non-linear rheology of two gelators in cyclohexane. Thixotropic loops for **STNO** (C=2.0 wt %) and **HSA** (C=2.0 wt %) gels in identical creeping conditions (**HSA**: σ/σ^*=0.59; **STNO**, σ/σ^*=0.56): TH_{STNO}=0.03173; TH_{HSA}=0.04781.

phenomenological and does not go into the analysis of the stress relaxation in SAFINs and the associated creep-recovery mechanisms. The maximum stress reached in the ascending segment is normalized by σ^* to allow comparisons. The area TH of the loops are TH_{HSA}=0.04781 and TH_{STNO}=0.03173 and shows that the creeping process is more important with **HSA** than with **STNO** gels. It therefore appears that a stiff and elastic gel can also creep more than a less 'solid-like' gel. The two properties relate, respectively, the linear and the non-linear viscoelasticities and characterize the elastoplasticity of the systems. The difference in TH can be accounted for by the chirality of the junction zones. The sliding of stacked ribbon-like fibers in **HSA**–cyclohexane gels appears to be more important than the disentanglement of intertwined **STNO** helical fibers, a mechanism that is clearly observed in TEM observations.[9]

To conclude on the elaboration of simplified methods to characterize complex materials like organogels, it is interesting to come back to their biphasic character. The sizes and shapes of the fibers, the mesh size of their networks, the proportion of junction zones, and other heterogeneities are intrinsic and non-homogeneous features of the systems

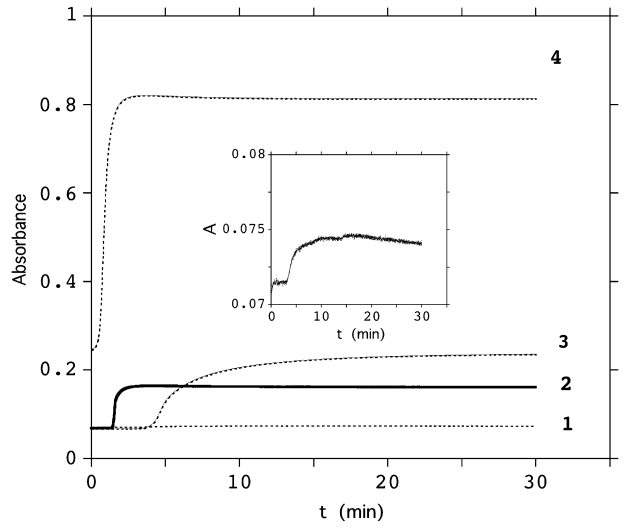

Figure 8. UV spectroscopy of the kinetics of formation of **HSA** gels (C=1.8 wt %) in different solvents at λ=550 nm (1 mm optical path length). **1**: toluene, **2**: dodecane, **3**: nitrobenzene, **4**: hexafluorobenzene. The inset is a close-up of the variation for the toluene gel.

that contribute to their crystalline-like nature. UV spectroscopy can probe the transmission of a light beam through the gels and Figure 8 illustrates the interest of such a simple method in comparing four different gels of the same gelator. The sequence of turbidity T is $T_{\text{hexafluorobenzene}} > T_{\text{nitrobenzene}} > T_{\text{dodecane}} > T_{\text{toluene}}$. The curve profiles confirm the fast kinetics of growth of the heterogeneities and its sequence, which is also that for the elasticities[36] and cross-sectional sizes of the fibers, as shown by previous scattering studies. The inset (Fig. 8) confirms that even for a visually transparent toluene gel, the sigmoid variation can be observed and the long equilibration confirmed. The mechanistic details of the role played by the solvent in the self-assembly process remain poorly understood although evidences for a solvent-assisted nucleation pathway inducing a rigidification of the 1D aggregates has been shown to influence the formation of bundles and/or gels in π-conjugated systems.[39]

3. Conclusions

Rheological properties of a paramagnetic, steroid-made organogel **STNO** are presented and carefully analyzed with respect to the conditions of observation of a linear viscoelastic regime. The scaling law G' versus concentration exhibits an exponent (ca. 2.0) commonly observed in the class of organogels. The information extracted from *simplified* SANS and rheological protocols is summarized in Table 1. It appears that the similar scaling observed for the two systems **STNO** and **HSA** suggests that similar physical concepts rule the properties and parameters: storage moduli G', thixotropic loops TH, cross-sectional areas of the rigid fibers A, mesh size ξ of the SAFINs, and kinetic equilibration time of the gel formation τ_{equ}. The linear elasticity depends on the solubility of the gelator, the mesh size of the related SAFIN, the Young's modulus of the material, and the cross-sectional size of the fibers. Thus, **HSA** organogels in cyclohexane have lower concentrations of non-aggregated gelators, larger mesh sizes, more homogeneous networks, and thicker fibers contributing to much larger elasticities compared to those from **STNO**. These differentiated properties make **HSA** gels more appropriate for applications where the 'solid-like' feature is important (e.g., lubricating greases)[40] or the homogeneity of the 3D networks (or their replicas) is determinant (e.g., for the diffusion of large species in filtration purposes).

The kinetics of aggregation reveals that the equilibration time is a long first order process as confirmed by rheological and scattering experiments. The transduction of the chirality from the molecular level (**HSA** has a single asymmetric center contrasting with the situation for the steroid **STNO**) to the supramolecular and higher hierarchical levels is also revealed by some non-linear viscoelastic properties of the gels (thixotropy). The steroid gels present lower creeping properties associated with the higher cohesiveness of the helical and super-helical nature of their junction zones. Such differences make the **STNO** system more appropriate than **HSA** for applications taking advantage of long characteristic times for the onset of the elastic modulus with limited deformations under mechanical stresses (e.g., specialized mechanical switches, shock absorbers). In general, SAFINs found in this class of 'reversible polymers' or molecular gels present a variety of rheological and thermodynamically controlled architectures that are tunable in a way not accessible to 'ordinary' polymers.[41]

The present study has taken the opportunity of the investigation of the flowing properties of a steroid organogel to analyze the normalization conditions allowing comparisons between different systems. SANS is used to evaluate the number density of fibers, their structural and kinetic features, while rheometry is used in a complementary manner to relate with the number density of elastically active fibrillar elements. The study proposes a simple methodology for reliable studies important for the elaboration of general concepts valid for SAFINs in molecular gels.

Although the present contribution illustrates how mechanical and structural properties of molecular gels can be stringently and conveniently evaluated (and partly correlated), it remains speculative to draw direct correlations

Table 1. Summary of the rheological and structural information gained from the simplified protocols as applied to the steroid (**STNO**) and fatty acid (**HSA**) organogels

Rheology			SANS		
G', σ^* scaling	$G'_{\text{HSA}}/G'_{\text{STNO}}$	$\text{TH}_{\text{HSA}}/\text{TH}_{\text{STNO}}$	$A_{\text{HSA}}/A_{\text{STNO}}$	$\xi_{\text{HSA}}/\xi_{\text{STNO}}$	$\tau_{\text{equ HSA/STNO}}$
C^2	2700	1.5	3.0	0.25	<0.5

The similar scaling observed for the two systems suggests that similar physical concepts rule the properties: storage moduli G', thixotropic loops TH, cross-sectional areas of the rigid fibers A, mesh size ξ of the SAFINs, kinetic equilibration time of the gel formation τ_{equ} (see text).

with the molecular structures of the gelators. To date,[3] it is still difficult to design molecules so that they will self-assemble to predefined structures and specific mechanical properties.

4. Materials and methods

The steroid gelator di-*n*-propyl-17,17 aza-17a D-homo(5α) androstanol-3β ($C_{25}H_{45}NO$) is a unique diamagnetic steroid (**STNH**) obtained from the enlargement of the D-ring and bears one amine function. It was synthesized according to the description given by Ramasseul et al.[42] The paramagnetic derivative **STNO** (Scheme 1) was obtained by oxidation of **STNH** using *m*-chlorobenzoic acid.[42] The racemic fatty acid **HSA** (12-hydroxy octadecanoic acid) was used as received from Aldrich.

SANS experiments were performed at the 30 m beam line of the National Center for Neutron Research of the National Institute of Standards and Technology, Gaithersburg, MD (λ=8.09 Å) using 1 mm path length quartz cells in a thermostatted (±0.1 °C) holder. Complementary experiments used the European neutron source of the Institut Laue Langevin (ILL, Grenoble, France) with the large dynamic range small-angle diffractometer D22. Deuterated cyclohexane was used to limit the incoherent scattering to that from the gelator molecules. The range of momentum transfer Q ($Q=4\pi/\lambda \sin\theta$, λ being the neutron wavelength and θ half the scattering angle) was $0.003\ \text{Å}^{-1}<Q<0.18\ \text{Å}^{-1}$. Standard corrections and calibration procedures were used to proceed with the radial averaging of isotropic 2D arrays of neutron counts collected on the detectors.[43] SANS kinetic experiments integrated the neutron counts on the 2D detector versus time during the **STNO** aggregation at a fixed sample-to-detector distance (14.4 m) and wavelength (6.00 Å) corresponding to $0.003\ \text{Å}^{-1}<Q<0.08\ \text{Å}^{-1}$ (translated detector by 0.450 m). The Q range surrounds the crossover regime between the low- and large Q asymptotic behaviors characterizing 1D species (see Q^* definition).

Rheometry measurements used a RS-600 controlled stress rheometer with a serrated plate–plate geometry (20 mm diameter) to limit the potentiality for sliding effects. The temperature was controlled within 0.1 °C. A glass cap filled with a saturated atmosphere of cyclohexane surrounded the measuring cell so that no solvent evaporation was distinguishable during the measurements. The **STNO** gel sandwich was formed externally and transferred at the equilibrium temperature (20.0 °C) on the stator except for kinetics experiments. Under these conditions, five G' measurements gave a total error bar of less than 20% ($G' = G'_0 \pm 10\%$).

The transmission electron micrograph measurements used an 80 keV JEOL 100C microscope with carbon replicas of a freeze-dried specimen as previously described.[9]

Acknowledgements

Dr. R. Ramasseul is especially thanked for the synthesis of **STNO** and for his continuous support. Prof. U. Maitra is acknowledged for having brought to our attention the need for a clarification about the use of rheometry for SAFINs. The NIST and ILL neutron facilities are acknowledged and in particular Drs. B. Demé and C. Glinka are thanked.

References and notes

1. Abdallah, D. J.; Weiss, R. G. *Adv. Mater.* **2000**, *12*, 1237–1247.
2. Terech, P. Low-molecular Weight Organogelators. In *Specialist Surfactants*; Robb, I. D., Ed.; Chapman and Hall: London, 1997; Chapter 8, pp 208–268.
3. *Molecular Gels: Materials with Self-Assembled Fibrillar Networks*; Weiss, R. G., Terech, P., Eds.; Springer: Dordrecht, The Netherlands, 2006; p 976.
4. Terech, P. *Encyclopedia of Surface and Colloid Science*; Dekker: New York, NY, 2002.
5. Tachibana, T.; Kitazawa, S.; Takeno, H. *Bull. Chem. Soc. Jpn.* **1970**, *43*, 2418–2421.
6. Tachibana, T.; Mori, T.; Hori, K. *Bull. Chem. Soc. Jpn.* **1980**, *53*, 1714–1719.
7. Tachibana, T.; Mori, T.; Hori, K. *Bull. Chem. Soc. Jpn.* **1981**, *54*, 73–80.
8. Terech, P.; Ramasseul, R.; Volino, F. *J. Phys. France* **1985**, *46*, 895–903.
9. Wade, R. H.; Terech, P.; Hewat, E. A.; Ramasseul, R.; Volino, F. *J. Colloid Interface Sci.* **1986**, *114*, 442–451.
10. Terech, P.; Ramasseul, R.; Volino, F. *J. Colloid Interface Sci.* **1983**, *91*, 280–282.
11. Lin, Y.-C.; Kachar, B.; Weiss, R. G. *J. Am. Chem. Soc.* **1989**, *111*, 5542–5551.
12. Furman, I.; Weiss, R. G. *Langmuir* **1993**, *9*, 2084–2088.
13. Brotin, T.; Utermöhlen, R.; Fages, F.; Bouas-Laurent, H.; Desvergne, J. P. *J. Chem. Soc., Chem. Commun.* **1991**, 416–418.
14. Murata, K.; Aoki, M.; Susuki, T.; Harada, T.; Kawabata, H.; Komori, T.; Ohseto, F.; Ueda, K.; Shinkai, S. *J. Am. Chem. Soc.* **1994**, *116*, 6664–6676.
15. De Loos, M.; Van Esch, J.; Stokroos, I.; Kellog, R. M.; Feringa, B. L. *J. Am. Chem. Soc.* **1997**, *119*, 12675–12676.
16. Ostuni, E.; Kamaras, P.; Weiss, R. G. *Angew. Chem., Int. Ed.* **1996**, *35*, 1324–1326.
17. Trivedi, D. R.; Ballabh, A.; Dastidar, P. *Cryst. Growth Des.* **2006**, *6*, 763–768.
18. Berret, J. F. Rheology of Wormlike Micelles: Equilibrium Properties and Shear Banding Transitions. In *Molecular Gels: Materials with Self-Assembled Fibrillar Networks*; Weiss, R. G., Terech, P., Eds.; Springer: Dordrecht, The Netherlands, 2006; p 667.
19. Terech, P.; Friol, S. *Macromol. Symp.* **2006**, *241*, 95–102.
20. Zölzer, U.; Eicke, H.-F. *J. Phys. II France* **1992**, *2*, 2207–2219.
21. Wierenga, A.; Philipse, A. P.; Lekkerkerker, H. N. W. *Langmuir* **1998**, *14*, 55–65.
22. Gradzielski, M.; Hoffmann, H.; Oetter, G. *Colloid Polym. Sci.* **1990**, *268*, 167–178.
23. Sollich, P.; Lequeux, F.; Hebraud, P.; Cates, M. E. *Phys. Rev. Lett.* **1997**, *78*, 2020–2023.
24. Terech, P.; Sangeetha, N. M.; Maitra, U. *J. Phys. Chem. B* **2006**, *110*, 15224–15233.
25. Callec, G.; Gauthier-Manuel, B.; Terech, P.; Ramasseul, R. *C. R. Acad. Sci. Paris* **1981**, *293*, 99–101.

26. Terech, P.; Dianoux, A.-J.; Ramasseul, R.; Volino, F. *C. R. Acad. Sci. Paris* **1981**, *293*, II749–II752.
27. Terech, P. *J. Colloid Interface Sci.* **1985**, *107*, 244–255.
28. Martinetto, P.; Terech, P.; Grand, A.; Ramasseul, R.; Dooryhee, E.; Anne, M. *J. Phys. Chem. B* **2006**, *110*, 15127–15133.
29. Larson, R. G. *The Structure and Rheology of Complex Fluids*; Oxford University Press: New York, NY, 1999.
30. Wu, H.; Morbidelli, M. *Langmuir* **2001**, *17*, 1030–1036.
31. Levine, A. J.; Head, D. A.; Mackintosh, F. C. *J. Phys.: Condens. Matter* **2004**, *16*, S2079–S2088.
32. Gibson, L. J.; Ashby, M. F. *Cellular Solids: Structure and Properties*; University Press: Cambridge, UK, 1997.
33. Leon, E. J.; Verma, N.; Zhang, S.; Lauffenburger, D. A.; Kamm, R. D. *J. Biomater. Sci. Polym. Ed.* **1998**, *9*, 297–312.
34. Jones, J. L.; Marques, C. M. *J. Phys. France* **1990**, *51*, 1113–1127.
35. Macintosh, F. C.; Käs, J.; Janmey, P. A. *Phys. Rev. Lett.* **1995**, *75*, 4425–4428.
36. Terech, P.; Pasquier, D.; Bordas, V.; Rossat, C. *Langmuir* **2000**, *16*, 4485–4494.
37. Terech, P. Small-angle Scattering and Molecular Gels. In *Molecular Gels: Materials with Self-Assembled Fibrillar Networks*; Weiss, R. G., Terech, P., Eds.; Springer: Dordrecht, The Netherlands, 2006.
38. Terech, P.; Rodriguez, V.; Barnes, J. D.; Mckenna, G. B. *Langmuir* **1994**, *10*, 3406–3418.
39. Jonkheijm, P.; Van Der Schoot, P.; Schenning, P. H. J.; Meijer, E. W. *Science* **2006**, *313*, 80–83.
40. Prost, J.; Rondelez, F. *Nature* **1991**, *350*, 11–23.
41. Sijbesma, R. P.; Beijer, F. H.; Brunsveld, L.; Folmer, B. J. B.; Ky Hirschberg, J. H. K.; Lange, R. F. M.; Lowe, J. K. L.; Meijer, E. W. *Science* **1997**, *278*, 1601–1604.
42. Martin-Borret, O.; Ramasseul, R.; Rassat, R. *Bull. Soc. Chim. Fr.* **1979**, *7–8*, II-401–II-408.
43. http://www.ncnr.nist.gov/, http://www.ill.fr/.